

# Hectochelle: a multi-object echelle spectrograph for the converted MMT

Andrew Szentgyorgyi, Peter Cheimets, Roger Eng,  
Daniel Fabricant, John Geary, Lee Hartmann, Mario Pieri, John Roll  
Harvard-Smithsonian Center for Astrophysics  
60 Garden St., Cambridge, MA 02138

## ABSTRACT

The Hectochelle will be a fiber-fed, multi-object spectrograph for the post-conversion MMT which will take 255 simultaneous spectra at a resolution of 32,000-40,000. The absolute efficiency, including optical fiber losses, is predicted to be 6%-10%, depending on the position of a line within a diffractive order. In one hour, features with 60 mÅ should be resolved in  $m_R = 18$  stars with a signal to noise of 10.

**Keywords:** Echelle spectrograph, high resolution spectroscopy

## 1. INTRODUCTION

The post-conversion Multiple Mirror Telescope (MMT) will have a 6.5 meter primary and a f/5 Cassegrain focus with a 1° full angle field of view (FOV) on a curved focal surface. A field corrector triplet, with atmospheric dispersion compensation, will deliver polychromatic point response functions (PSFs) with 90% encircled energy diameters of 0.6 arcsec over this FOV (Fabricant *et al.*, 1994). Two fiber fed spectrographs, Hectospec and Hectochelle, are being built to exploit this unique platform for multi-object spectroscopy. While Hectospec (Fabricant *et al.*, 1994) is a moderate dispersion spectrograph operating at resolutions of 1,000 to 5,000, the Hectochelle will be an echelle spectrograph operating at resolutions from 32,000 to 40,000 suited to stellar radial velocity surveys and detailed spectroscopic studies. Both spectrographs will be fed with the same focal plane robot positioner which positions optical fiber ends over the 1° focal surface.

Since the dimension perpendicular to dispersion on the spectrograph focal plane is used to distinguish the individual fiber ends, cross-dispersion is precluded; the Hectochelle will be a single-order instrument. A single diffractive order is selected by means of narrow band interference filters on an automated filter changer. While 300 fibers will be available in the fiber bundle, we have chosen to sacrifice some multiplex advantage to improve resolution; Hectochelle collects 255 spectra simultaneously.

## 2. OPTOMECHANICAL DESIGN

The optical design is shown schematically in Figure 1 and a isometric view of the spectrograph appears in Figure 2. The spectrograph will quite large; the grating and camera mirror are separated by 4.26 meters and the optical bench will be 1.1 meter by 5.2 meters

The “slit” of the spectrograph is a linear arrangement of the fiber ends held in the optical fiber “shoe” or feed. The slit is curved and lies on a circle that is concentric with the collimator mirror center of curvature, *i.e.*, the slit obeys the Schmidt symmetry condition. The fibers are 250μm in diameter, which is a good match to the plate scale (170μm/arcsec) and PSF of the MMT telescope.

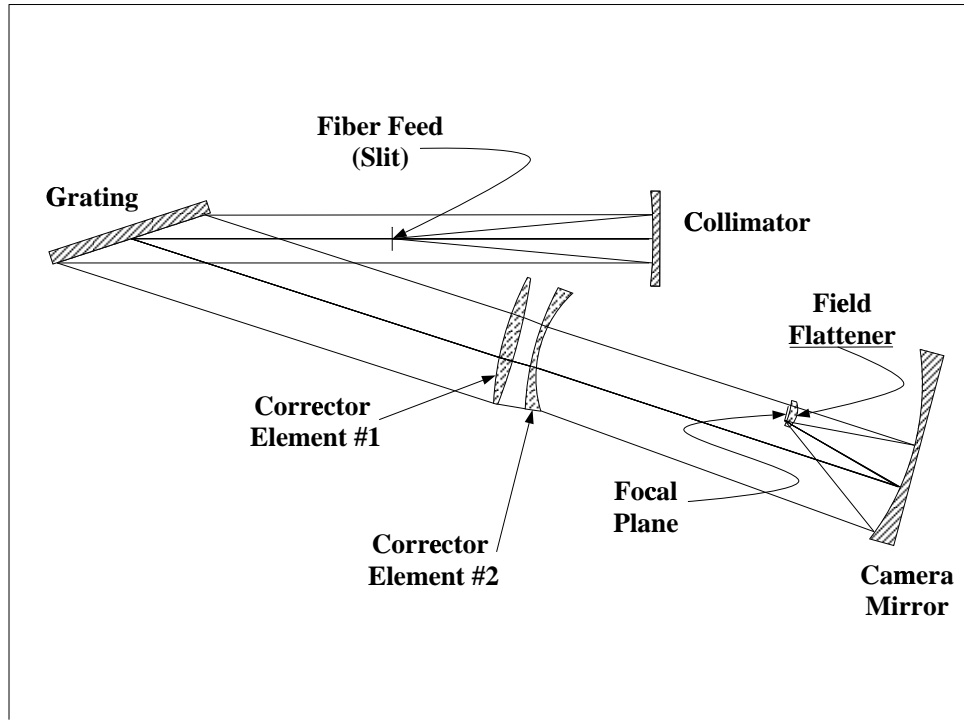


Figure 1: Optical Layout of Hectochelle Spectrograph. All surfaces are spherical. All refractive elements are fused silica.

The order-separating filter passband width will usually be a free spectral range (typically  $\Delta\lambda = 100\text{-}150 \text{ \AA}$ ), however filters with wider, multi-order passbands may be preferable for some purposes, such as studies of emission line objects. The effect of finite focal ratio on the bandpass of the interference filters is negligible.

The filters will be segmented into three parts to match better the curvature of the slit (fiber shoe). We have considered other possible locations for the order separating filter, and the only other possible location where the beam is small enough to separate orders with reasonably sized filters is immediately in front of the camera field flattener. At this point the beam is  $f/0.7$ , so the cone angle of the beam would significantly affect the passband of the interference filters.

The filters will be introduced into the beam with a mechanized filter changer that can be commanded from the observer console. The filter changer resembles a manual typewriter mechanism (see the Figure 3), where the small filters take the place of the impact head and filters are moved in and out of the beam by a cam-follower (see detail in Figure 3). The changer holds 30 filters simultaneously which spans the orders of the spectrograph over its usable passband.

The focal length of the spherical collimator mirror is 1371 mm. The  $f/5.3$  beams that emerge from the fibers are collimated to a 259 mm diameter parallel beam. The collimator will be made of Zerodur and is 584 mm in diameter. The beam then passes back over the optical fiber shoe, so considerable effort has been expended to minimize the fiber shoe cross-section to the return beam, while maintaining a rigid support structure for the fibers.

The grating we require for Hectochelle is too large to be ruled monolithically, so it will be necessary to mosaic two smaller gratings. The two gratings, ruled by Richardson Grating Lab, have 302 mm by 410 mm ruled surfaces, forming 835 mm by 302 mm mosaic grating with a 15 mm dead band down the middle of the mosaic. This dead band, which is parallel to the rulings, arises in part from the ruling process itself and from the requirement for a mechanical clearance between the grating substrates. The dead band will be minimized by pistoning one grating with respect to the other, thus throwing part of the dead band into the shadow of the other grating. The design

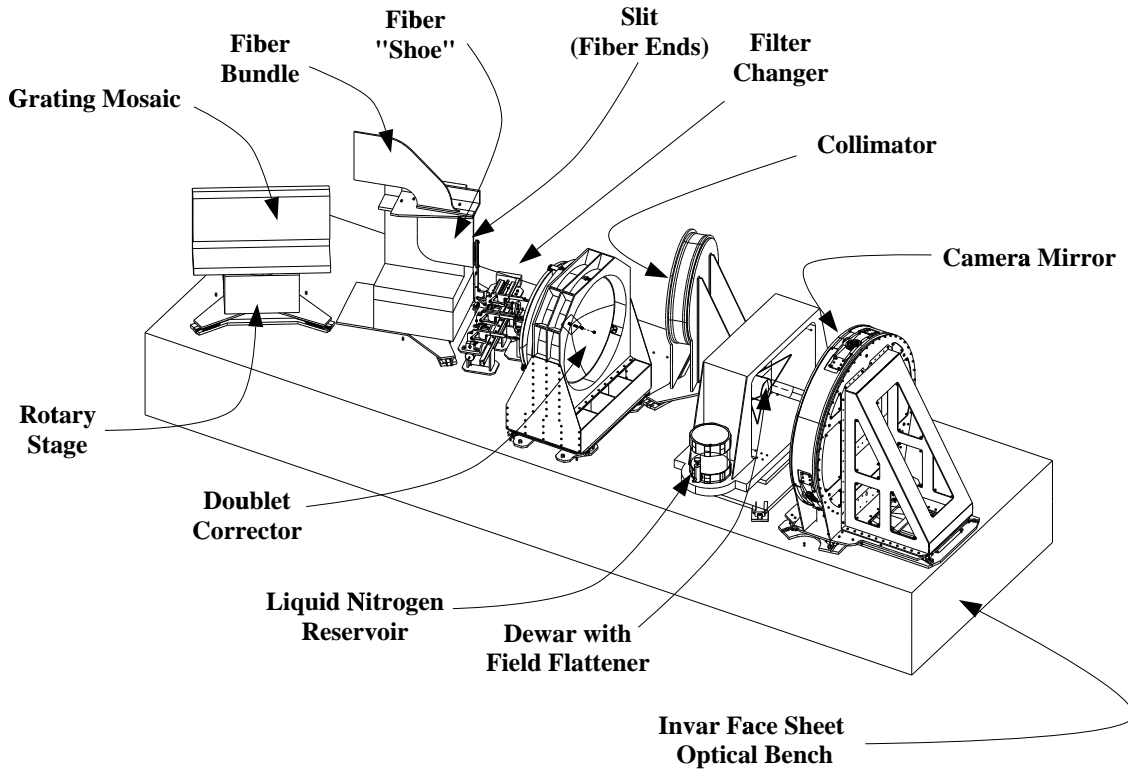


Figure 2: Isometric view of Hectochelle spectrograph.

of the grating cell is the subject of another contribution to these proceedings (Cheimets, *et al.*, 1998). The ruling pitch of these gratings is 110 lines per millimeter (lpm) and they are blazed at  $64.5^\circ$ . The grating mosaic will be operated at a nominal angle of incidence of  $72^\circ$ . The opening angle between the incident and diffracted beam is  $15^\circ$  to provide adequate clearance between the beams and the spectrograph optical elements and support structures. In this configuration, the spectrograph produces the “pseudo-echellogram” which appears in Figure 4, where the various orders appear as if they were cross-dispersed. In this diagram, the edges of the CCD format are indicated with dotted lines. Since a free spectral range becomes larger than the CCD format at  $5000\text{\AA}$ , it is necessary to tilt the grating to provide full spectral coverage. For this reason the grating will be mounted on a rotary stage with 1 arcsec (5 pixel) accuracy. The gratings will be aluminum coated.

The doublet corrector has been designed by Harland Epps and is a variant of the design used in several other large format spectrograph cameras, *e.g.* HIRES (Vogt, *et al.* 1994) and Hectospec. The refractive doublet corrector is an all-spherical design with silica elements. The lenses are quite large (692 mm and 659 mm diameter) and the support design is constrained somewhat by a requirement that the support not vignette the collimator-grating beam. The lens will be supported in a cantilevered tangential flexure design that borrows from the Hectospec design (see Figure 5). Although this support, and all the other supports in the spectrograph, will be made of steel to control cost, the design is athermalized with tangential flexures.

The camera mirror is spherical, F/0.7 and quite large ( $\sim 1.1$  meter diameter). The size of this mirror was driven by a desire to share the fiber shoe (and positioner robot) with the Hectospec instrument, while preserving the high resolution of the spectrograph. The mirror substrate will be Zerodur and the aspect ratio (diameter to thickness at vertex) is 25:1, but the ratio of edge thickness to diameter is 8:1. While the fast focal ratio would seem to compound the difficulty of fixturing a mirror with an aspect ratio this high, the depth of the sagitta makes the edge of the mirror very stiff. The mirror can be polished to specification without the use of exceptional metrology or polishing fixtures. Zerodur has a high stiffness-to-density ratio, when compared with silica or ULE, so it is an optimal choice for this design. The mirror is supported on titanium tangential flexures through nubs bonded to the mirror, so the design is

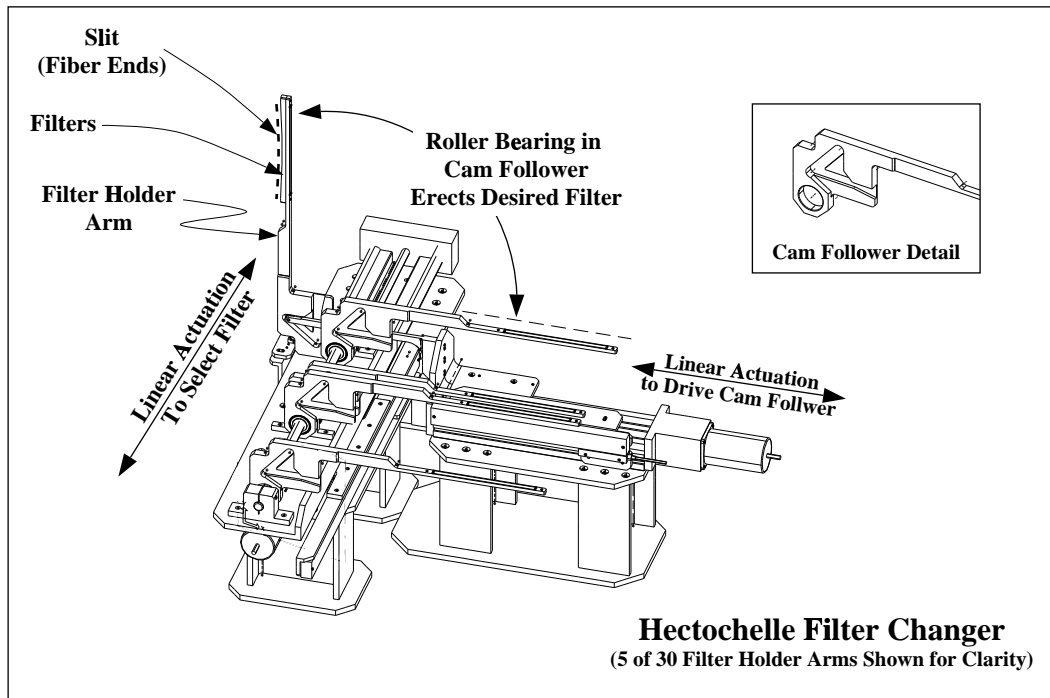


Figure 3:

also athermal (see Figure 5). The gravity induced deformations in this mount are less than  $\frac{1}{32}\lambda$  root-mean-squared (RMS) for surface deformations of order higher than focus (*i.e.*, curvature).

The camera is an internal focus system that is supported with a tensile spider and a thin, vacuum-jacketed cold finger. The field flattener is also a bispherical convex-concave, silica element that also serves as the vacuum window of the dewar. The focal plane consists of a mosaic of two  $2k \times 4.5k$  pixel CCD's manufactured by EEV, Ltd. These devices, which will be used in Hectospec and Megacam, have  $13.5\mu\text{m}$  pixels and will be backside illuminated for high quantum efficiency and good blue response. While these devices are essentially four-edge buttable, there is a 1 mm dead band between the two CCDs. The dead band is parallel to the dispersion direction, so a gap is introduced into the arrangement of the fibers in the shoe to guarantee that no fiber falls in this crack. The CCD's are discussed more fully in the context of the Megacam project elsewhere in these proceedings (McLeod, *et al.*, 1998).

The paraxial magnification of the spectrograph is 0.45, and the anamorphic factor is 0.57, so the nominal width of a spectrograph resolution element (the image of a  $250\mu\text{m}$  fiber end) is  $63.8\mu\text{m}$ , or 4.7 pixels. The image of a fiber end, which defines a resolution element, is an ellipse which is narrower in the dispersion direction than the fiber fan out direction by an amount given by the anamorphic factor, *i.e.*, the axial ratio of the ellipse is equal to the anamorphic factor. Each spectrum is 9.3 pixels wide perpendicular to dispersion, but this dimension is projected out in data reduction. When the projection of the elliptical image of the fiber end onto the dispersion axis is considered properly, the resolution element is slightly smaller than the minor axis of the elliptical image, even when the finite point response of the spectrograph is included. The resolution element will be slightly smaller than the nominal value. The point response, shown for a typical operating configuration in Figure 7, never exceeds  $14\mu\text{m}$  RMS radius.

The room which houses the both the Hectospec and Hectochelle spectrographs will be well insulated but unheated, so it will track the mean nighttime dome temperature. Temperature changes will be less than  $0.25^\circ\text{F}/\text{hour}$ , so thermal gradients will be quite small. Nonetheless, we may expect operating temperature to range from  $10^\circ\text{F}$  to  $70^\circ\text{F}$ , so it is essential to athermalize all the optical support and interface designs. We have selected an Invar optical bench with Invar face sheets that have a measured coefficient of thermal expansion (CTE) of  $\sim 1.3 \times 10^{-6}/^\circ\text{C}$  so as to minimize deformations of the bench resulting from a thermal gradient between the top and bottom face sheets. These

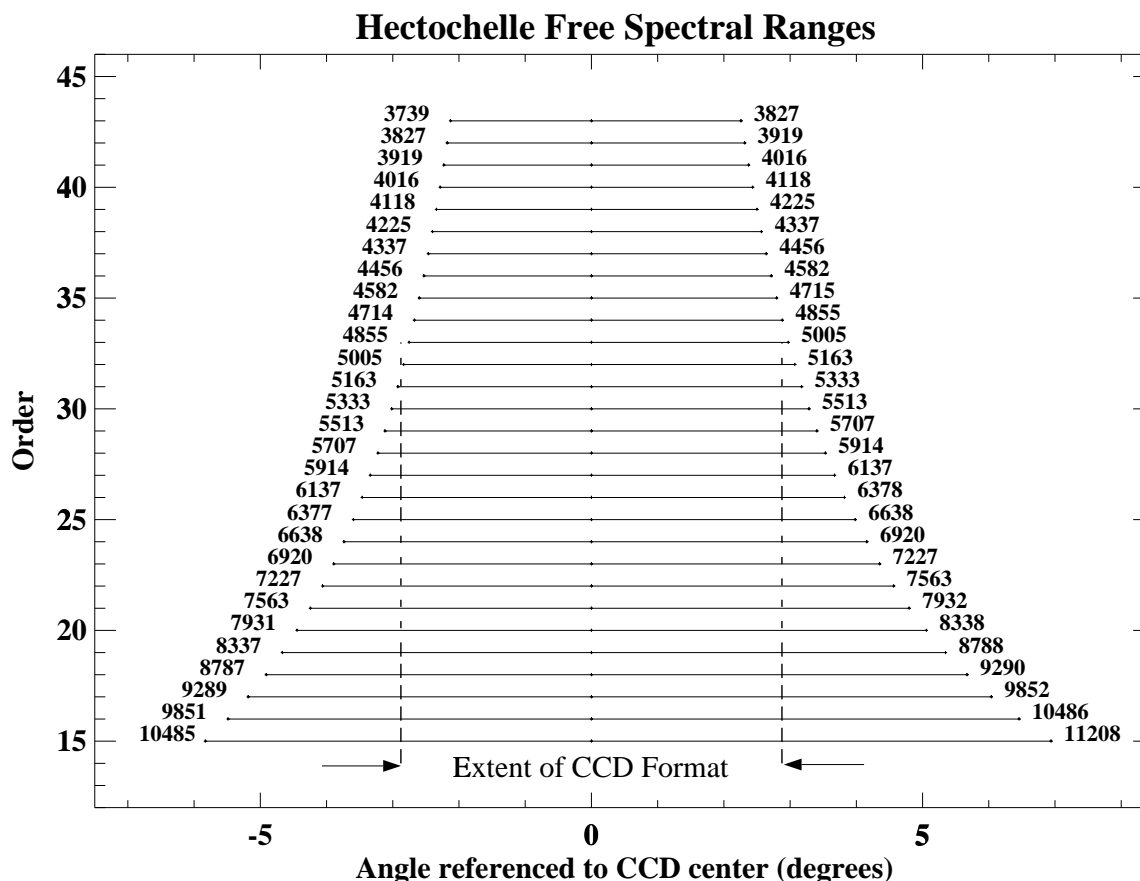


Figure 4: The pseudo-echellogram indicates angular extent of diffractive orders over the usable passband of the Hectochelle. The wavelengths, in Å, at the ends of each free spectral range are printed at the end of each order. The edge of the CCD format is indicated with vertical dotted lines.

deformations, like those of a bi-metal strip, bow the bench and tilt all the optical elements. The use of Invar for the optical mounts is costly and unnecessary; we have athermalized not only the optical mounting interface but the interface to the optical bench with a three-rail system (except the camera mirror, which employs a six-rail system). This support system, designed by Robert Fata (see Fata *et al.*, 1998 for a fuller discussion) for the Hectospec optical mounts, consists of THK linear slider rails mounted to the optical bench in a radial pattern centered on the vertex or null point of the optical element (see Figure 6). Although the mount itself may undergo conformal expansion and contraction, the motion of the vertices of all the optical components of the spectrograph is governed by the small CTE of the Invar face sheets. The optical mount materials that determined the vertical alignment of the optical elements are carefully matched to guarantee that the thermally induced motions of the vertices in the vertical direction are conformal.

#### 4. Spectrograph Efficiency and Resolution

Efficiency and resolution are the key parameters of the spectrograph design. The fixed contributors to the spectrograph efficiency are tabulated in Table 1 and plotted in Figure 8. In Table 1, the mirror reflectivity is calculated for two surfaces of dielectrically enhanced and protected silver which may have 0.976 to 0.994 reflectivity between 3800Å and  $\geq 1.1\mu\text{m}$ . The fiber internal transmission is derived from direct measurement of a sample of the fiber that will be used for the Hectochelle/Hectospec and is discussed in another contribution to these proceedings (Fabricant *et al.*, 1998). The external fiber efficiency includes the focal ratio degradation and reflections at the ends of the fiber. In the passband of the spectrograph, lens transmission of three refractive elements is governed by the six air-glass

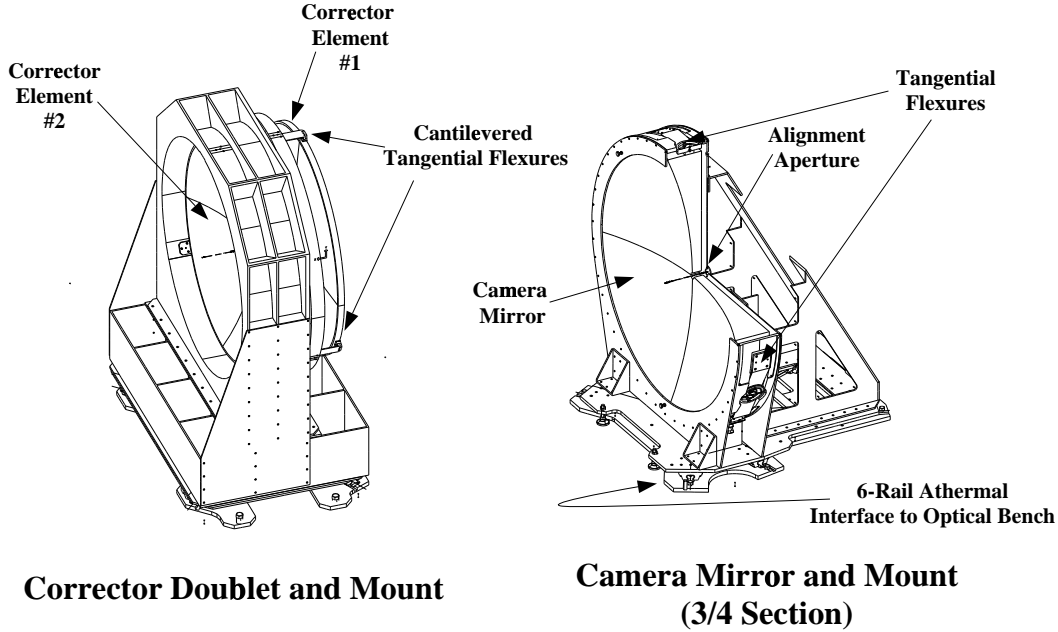


Figure 5: Isometric views of corrector doublet and camera mirror in mounts. Camera mirror is shown in 3/4 section to show tangential flexures.

interfaces. The losses at these interfaces have been substantially reduced with Sol-gel antireflection coating, which is discussed in some detail in another contribution to these proceedings (Bohn, 1998). Vignetting losses result from the obscurations of the fiber shoe, the internal focus camera and the dead band between the two grating mosaic elements.

There are several other contributors to losses in the spectrograph which depend on the operating configuration of the spectrograph. The transmission of the order-separating filters will depend principally on the width of the filter passband, varying from 0.35 peak transmission at Ca II ( $\lambda 3933$ ) to over 0.50 transmission in the 5000-7500Å band.

The efficiency of the grating itself depends on the diffraction angle, the angle of incidence and the reflectivity of the aluminum coating. For angles of incidence greater than  $72^\circ$ , the grating is over-filled, so there is a small additional loss due to a portion of the spectrograph beam falling off the ends of the grating. The observer has the flexibility to locate an atomic line of interest anywhere on the CCD format, with consequences for efficiency and resolution that vary on a line-by-line basis. In Figure 10, the absolute efficiency and resolution at Ca K  $\lambda 3933$  and Na D  $\lambda 5895$  are shown. All contributing factors have been included in the efficiency calculation. It can be seen that efficiency and resolution may, in some cases, depend critically on the angle of incidence. Furthermore, it is possible to achieve resolutions over 40,000, generally at the expense of a modest amount of efficiency.

## 5. EXPECTED SCIENTIFIC PERFORMANCE

The multiplex advantage of a multi-object spectrograph is only realized for studies of objects that are clustered or have a high surface density on the sky. Hectochelle will be a powerful tool for studying open and globular clusters, as well as the constituents of nearby local group dwarf galaxies.

One of the important uses of high-resolution astronomical spectroscopy is the measurement of radial velocities in systems with small velocity dispersions, such as binary stars, open and globular clusters, and dwarf galaxies. For example, in a one hour exposure Hectochelle should be able to measure the radial velocity of a typical low-mass star to an accuracy of 100 m/s at  $m_V = 17.5$  or an accuracy better than 1 km/s at  $m_V = 20$ . At these magnitude limits

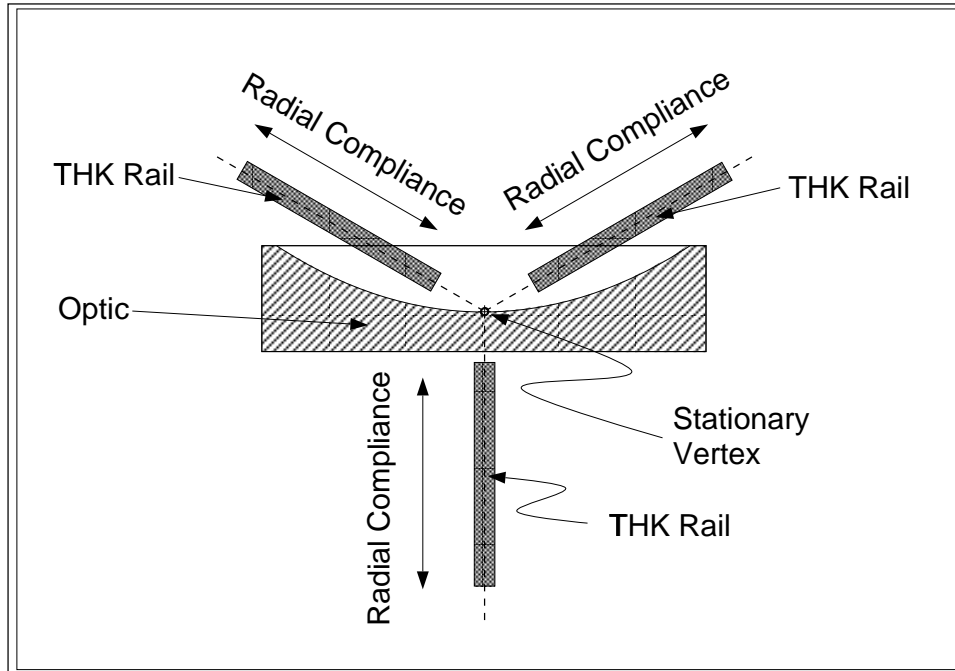


Figure 6: The athermal interface between the steel optical mounts and the Invar optical bench face sheet. The THK rails allow thermal expansion and contraction of the mounts without distorting the Invar face sheet. The rail are arranged in a radial pattern centered on the vertical axis through the element vertex, so the optical surface remains stationary over thermal cycles.

Hectochelle can simultaneously observe several hundreds of stars in clusters like the Pleiades, delivering both the throughput and multiplex advantage needed to make studies of cluster dynamics practical.

As an example of the scientific power of Hectochelle, we calculate the spectrograph performance in a passband including  $\text{Li } \lambda 6707$ . Lithium abundances are the focus of considerable astrophysical interest, but progress on this problem has been hindered by the weakness of the lithium feature in metal poor stars, with equivalent widths as low as  $10 \text{ m}\text{\AA}$ . In Figure 11, we plot the signal-to-noise as a function of equivalent width we would expect in a 1 hour exposure. This calculation as repeated for a sequence of stellar magnitudes in a range of  $m_R = 16 - 21$ . With Hectochelle, it will be possible to reach extremely faint magnitude and small equivalent widths for a extremely large sample of stars.

## ACKNOWLEDGMENT

We thank Robert Fata and Edward Hertz for sharing the the results of Hectospec design studies. We thank Harland Epps is responsible for the optical design of the camera. We also thank Steve Vogt and Bruce Bigelow for their advice and criticism, particularly as regards the design of the grating mosaic. William Davis and David Caldwell, through their designs and analyses for Hectospec have contributed to this project. Ying Zhou was responsible for the early phases of the mechanical designs discussed in this paper.

## References

Bohn, J.H. (1998) "*Sol-gel antireflective coatings for astronomical optics*", These proceedings #3355-63.

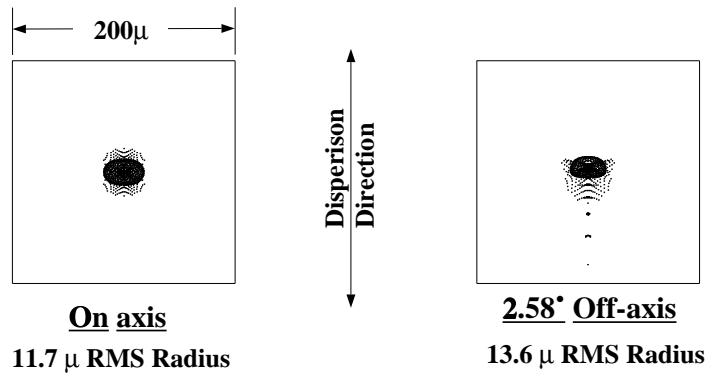


Figure 7: Spot diagram for Hectochelle on-axis and  $2.58^\circ$  off axis. This corresponds to the edge of the CCD format.

Cheimets, P., Szentgyorgyi, A.H., Pieri, M.R. (1998) “*Mosaic echelle grating support for the Hectochelle spectrograph*” These proceedings, #3355-108.

Fabricant, D.G., Hertz, E.H., Szentgyorgyi, A.H., Fata, R.G., Roll, J.B., Zajac, J. (1998) “*Construction of the Hectospec: a 300 optical fiber-fed spectrograph for the converted MMT*” These proceedings, #3355-60.

Fabricant D.; Hertz, E.; and Szentgyorgyi, A. (1994) “*Hectospec: A 300-Optical-Fiber Spectrograph for the Converted MMT.*” in *Instrumentation in Astronomy VII*, Proceedings of SPIE, vol. 2198, eds. D. L. Crawford and E. R. Craine, p. 251. (Bellingham, Washington: SPIE).

Fata R. and Fabricant, D. (1998) “*Mounting large lenses in wide-field instruments for the converted MMT*” These proceedings, #3355-59

McLeod, B.A., Geary, J.C., Gauron, T.M., Ordway, M.P. (1998) “*Megacam: paving the focal plane of the MMT with silicon*” (1998) These proceedings, #3355-26.

Vogt, S.S., *et al.* (1994) “*HIRES: the high resolution echelle spectrometer on the Keck 10-m Telescope*” In *Instrumentation in Astronomy VII*, Proceedings of SPIE, vol. 2198, eds. D. L. Crawford and E. R. Craine, p. 362. (Bellingham, Washington: SPIE).



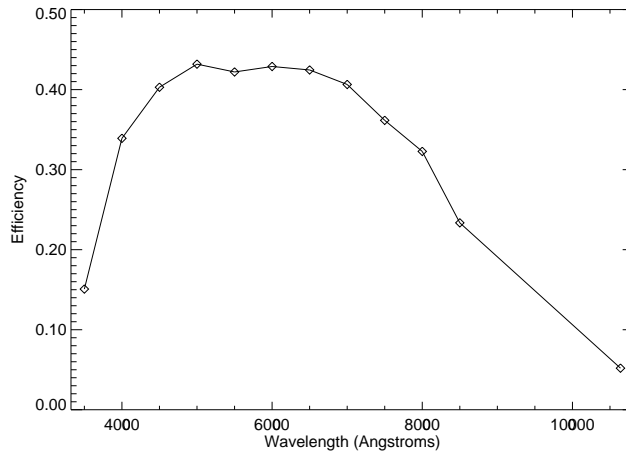


Figure 8: Efficiency vs. Wavelength for fixed contributors to the efficiency of the spectrograph, *i.e.*, exclusive of grating losses.

$\lambda$	Mirror Refl.	CCD Q.E.	Fiber Int. Tran	Fiber Ext. Eff.	Lens Trans.	Vign.	Eff. Q.E. ( $\xi_{fixed}$ )
4000	0.96	0.80	0.80	0.80	0.92	0.75	0.34
4500	0.97	0.83	0.86	0.80	0.97	0.75	0.40
5000	0.96	0.85	0.90	0.80	0.98	0.75	0.43
5500	0.94	0.83	0.92	0.80	0.98	0.75	0.42
6000	0.97	0.80	0.94	0.80	0.98	0.75	0.43
6500	0.95	0.80	0.95	0.80	0.98	0.75	0.42
7000	0.96	0.75	0.96	0.80	0.98	0.75	0.41
7500	0.97	0.67	0.96	0.80	0.96	0.75	0.36
8000	0.97	0.60	0.97	0.80	0.95	0.75	0.32
8500	0.97	0.45	0.98	0.80	0.91	0.75	0.23

Table 1: Efficiency of Hectochelle Spectrograph vs. Wavelength. Fiber losses are divided into internal attenuation over a 26 meter fiber length and external effects, the latter including focal ratio degradation reflection losses at ends and non-telecentricity. Grating losses are not included in these calculations.

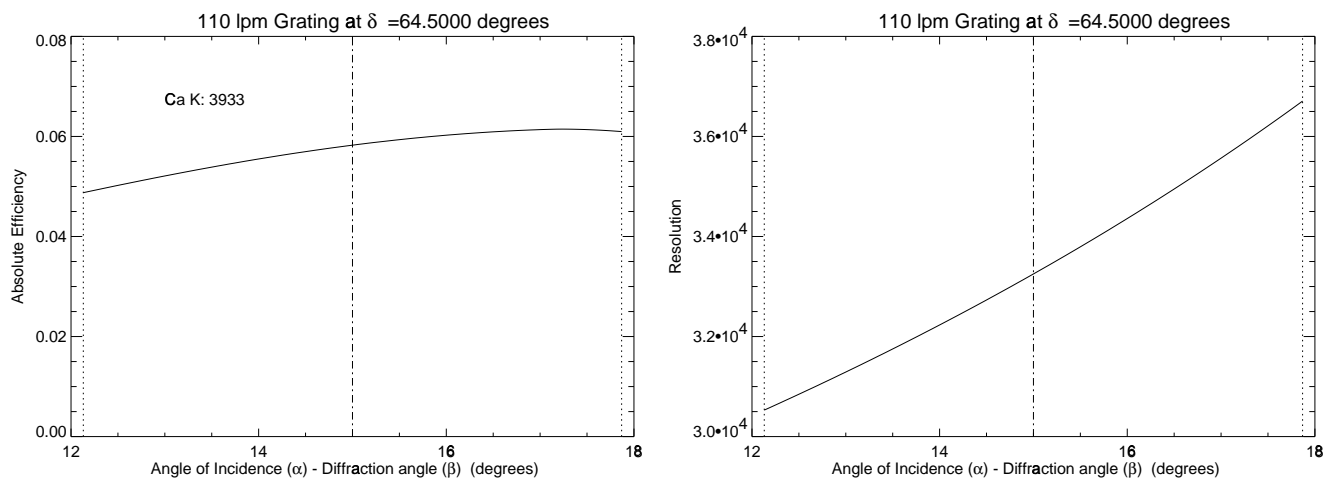


Figure 9: Hectochelle Efficiency and Resolution at Ca K ( $\lambda 3933$ ). Edges of CCD format are indicated with dashed lines, center indicated with dot-dash.

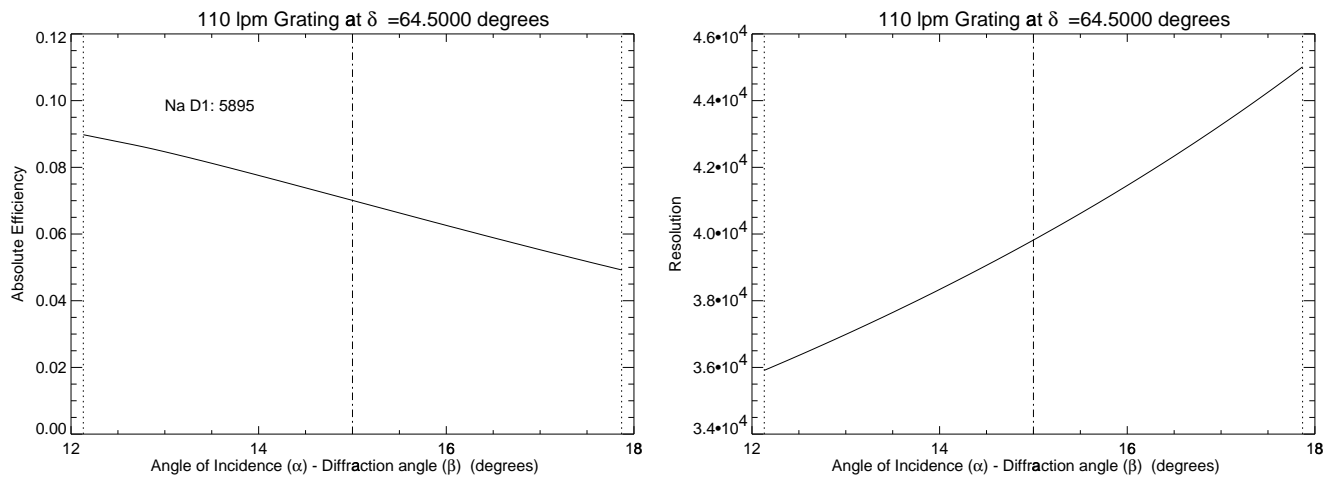


Figure 10: Hectochelle Efficiency and Resolution at Na K ( $\lambda 5895$ ). Edges of CCD format are indicated with dashed lines, center indicated with dot-dash.

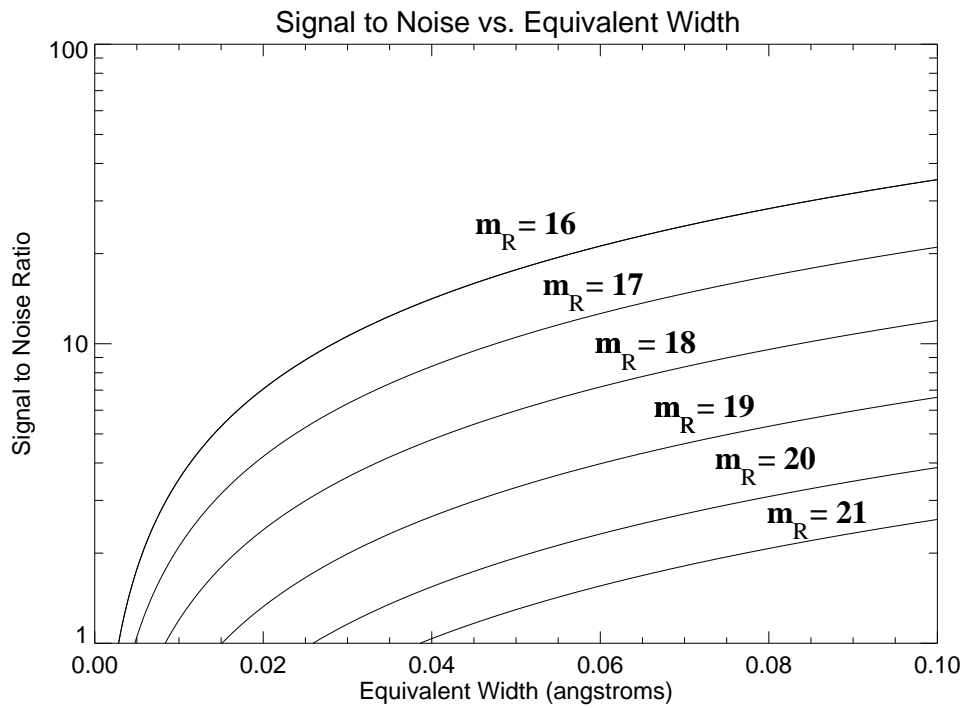


Figure 11: Signal to noise as a function of line equivalent width for 1 Hour Hectochelle exposure in dark time for star of various magnitudes